

No. 112/19, 23–34  
ISSN 2657-6988 (online)  
ISSN 2657-5841 (printed)  
DOI: 10.26408/112.02

Submitted: 23.06.2019  
Accepted: 24.07.2019  
Published: 30.12.2019

## IMPACT OF AIR FUEL MIXTURE FORMATION METHOD ON SOOT EMISSION VOLUME IN SHIP ENGINE EXHAUST GAS

**Dmitry Glazkov**

Baltic Public Fishery Academy, Kaliningrad University of Technology, 6 Molodyozhnaya,  
236035 Kaliningrad, Russia, Faculty of Ship Engines,  
e-mail: 2338697@gmail.com

**Abstract.** The paper discusses the mechanism and properties of the soot generation process for cases of volumetric and volumetric/film-based methods of air fuel mixture formation. Results of testing the impact of operating factors on soot emissions are shown. For selected ship engines, empirical relations between soot emissions and affecting factors are determined.

**Keywords:** Ship combustion engines, soot generation, hard coal particles.

### 1. FOREWORD

Complete combustion of fuel injected to a cylinder is hindered by time limits of the processes occurring inside cylinder, as well as their inefficiency, uneven distribution of oxygen and fuel within the cylinder, and others. With a local shortage of oxygen and high temperatures of the medium in the cylinder, the injected fuel is pyrolysed and incomplete oxidation products are generated: carbon monoxide, aldehydes, carboxylic acids, soot, various heavy hydrocarbons, generally aromatic ones of the naphthalene type with large numbers of condensed rings and multiple bonds [Broze 1969; Dyachenko et al. 1974].

### 2. SOOT GENERATION MECHANISM

The soot generation process is divided [Broze 1969] into three stages: nucleus formation, nucleus growth into soot particles, and coagulation of soot particles. Soot generation rate is determined by the rate of the chemical processes occurring during fuel pyrolysis. A diagram of soot generation mechanisms (paths) according to Prof. D.D. Broze [Broze 1969] is shown in Figure 1.

During the induction period, at temperatures within the cylinder in the order of 1000–1500 K, polycondensation and polymerisation reactions generally occur. Under such conditions, the nuclei can be cycloparaffins and hydrocarbons with multiple bonds in their molecules. The reactions occur with a breaking of rings and multiple bonds. At local temperatures of 2000 K and above [Broze 1969; Dyachenko et al. 1974], suitable for the combustion process in the engine cylinder, dehydrogenation reactions occur first.

The higher the molar mass [Kavtaradze 2008; Odintsow and Glazkov 2014] of straight-chained saturated and unsaturated hydrocarbons, the higher the rate of soot particle generation. These deposits are soluble in carbon disulfide, which indicates the presence of aromatic rings and carbonyl groups.

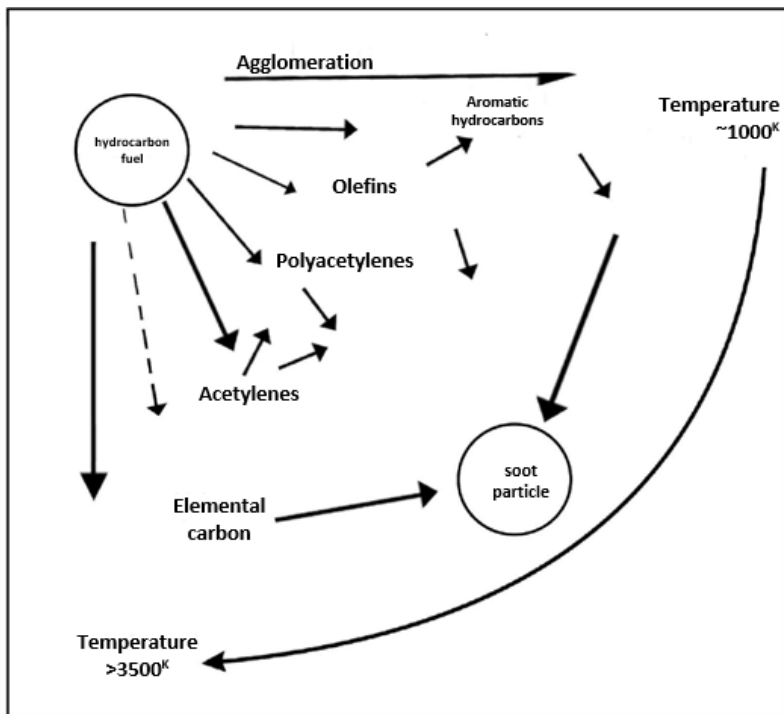


**Fig. 1.** Diagram of soot generation paths according to Prof. D.D. Broze [Broze 1969]

The value of the local excess air ratio  $\alpha$  at which soot begins to be released from the flame depends on several factors: air temperature and pressure in the cylinder, thermal physical properties of the fuel, as well as the quality of its atomisation, and falls within the range 0.33–0.7. With increasing temperature, soot formation initiation changes in the direction of reducing the excess air ratio, and with increasing pressure – in the direction of increasing the factor. This is shown in Figure 2.

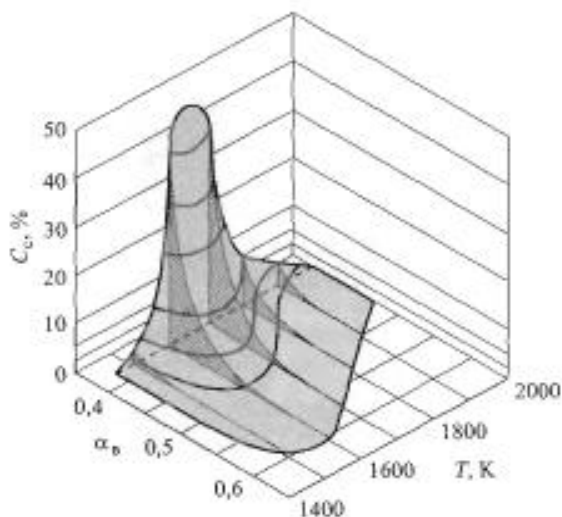


**Fig. 2.** Relation between soot concentration and local excess air ratio and temperature inside the cylinder according to [Kavtaradze 2008]

Concurrently with soot generation, soot combustion in reactions with oxygen and hydroxide groups occurs. Soot combustion rate depends in its particle diameter [Broze 1969]: soot in a flame has sufficient time to combust fully if its particle diameter is no greater than several  $\mu\text{m}$  (micrometres). Soot combustion occurs at the end of the combustion process, at the afterburning section. Therefore, the heat generated during soot combustion is used ineffectively in the cylinder. Its effective use is only possible outside the cylinder: in a turbine or a waste heat boiler.

The soot generation process in combustion engines also depends on the method of air fuel mixture formation. In engines with mainly volumetric air fuel mixture formation, fuel is fed to the cylinder as a stream containing  $10^7$  droplets with diameters of 1 to 300  $\mu\text{m}$  and greater. According to numerous studies [Bratkov 1985], flame spreads on the external surface of the fuel stream and within approx. 0.5 ms covers the entire surface. The fuel stream surface is therefore a boundary of heat and mass exchange between fuel fed to the cylinder and the air medium.

In engines with film-based and film/volumetric air fuel mixture formation, part of the circulated fuel does (from 50 to 95%, depending on the combustion chamber design) is fed to the bottom of the piston and evaporates from there. In exchange, the combustion chambers in such engines are filled in the cylinders. A piston design with a CNIDI combustion chamber, used in the 6CZN18/22 “Khabarovets” engine is shown in Figure 3 [Dyachenko et al. 1974].

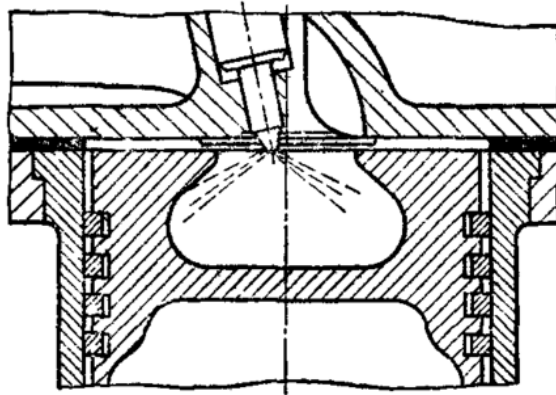


**Fig. 3.** Combustion chamber of the 6CZN18/22 "Khabarovets" engine

At the bottom of the piston, the fuel gathers in the form of large droplets, as small droplets, which do not reach the piston surface, are caught by the rotating air charge. Under such conditions, the fuel evaporation process depends on the rate of heat exchange between the fuel film and the piston surface. For particularly cool piston bottom surfaces, when their temperature does not exceed 90% fuel boiling point [Kamfer 1974], fuel flows freely along the surface. The heat exchange process in this case is very similar to heat removal during bubble boiling. At higher temperatures, a layer of vapour forms between fuel and the cylinder walls, which greatly inhibits heat exchange and slows down evaporation. This fact, combined with low air speeds in the boundary layer, leads to a local shortage of oxygen, and to fuel pyrolysis with deposition of soot and lacquer films at the piston bottom. The lacquer and soot layers have a thermal conductivity two orders of magnitude lower than the thermal conductivity of the piston material [Kavtaradze 2008]. This causes a local overheating and degradation of metal microstructure, up to a formation of cracks and piston burnout.

### 3. SOOT EMISSION PROCESS TESTING

As an indicator of the quality of fuel evaporation from the combustion chamber wall surface, relative fuel film area can be used [Odintsow 2010]:

$$K_p = F_b/g \quad (1)$$

where:

$F_b$  – is the fuel film surface area,

$g$  – is the part of the cycle fuel dose trapped during injection on the combustion chamber walls.

With increasing cycle dose, naturally, fuel stream length increases. For this reason, in some engines with predominantly volumetric air fuel mixture formation, a portion of the cycle fuel dose reaches the combustion chamber surface when the engine operates close to full power. The film-based mixture formation mechanism adds to the volumetric one. However, unlike engines with predominantly film-based air fuel mixture formation, fuel evaporation occurs in less favourable conditions, from a relatively cool surface. These circumstances cause increased soot emissions [Odintsov and Glazkov 2014; 2016]. The relations between measured soot emissions and indicated power on load curves (at constant RPM) for selected engines are shown in Figures 4–6.

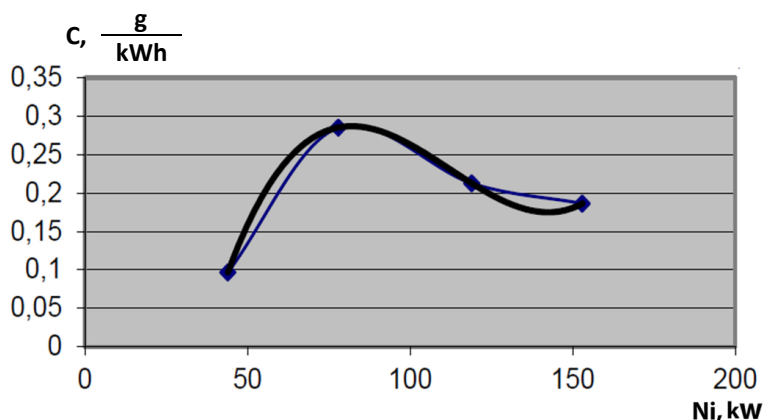


Fig. 4. Measured soot emission to indicated power relation for the 6CZN 18/22 “Khabarovets” engine ( $n = 750$  RPM)

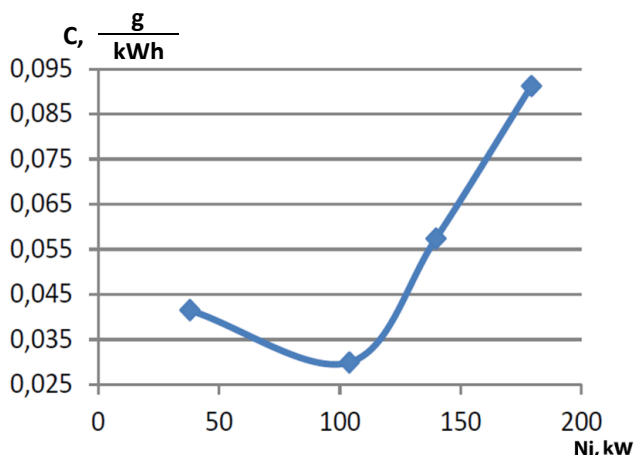
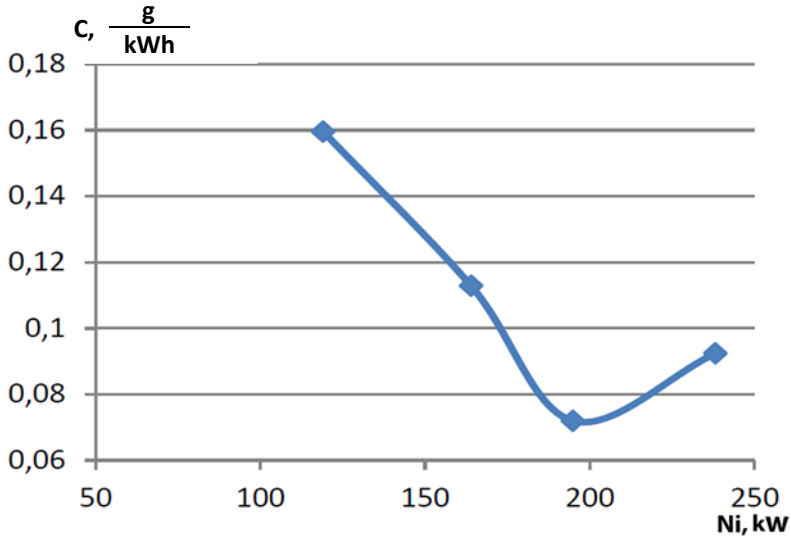


Fig. 5. Measured soot to indicated power relation for the MAN D 2866 LXE engine (cylinder diameter  $D = 128$  mm, piston stroke 155 mm,  $n = 1500$  RPM)



**Fig. 6.** Measured soot to indicated power relations for the 3D6 engine (6CZ 15/18, n = 1900 RPM) [Medvedev 2016]

To determine the impact of engine design and technical condition on the process of generation, combustion and emission of soot, the results presented in Figures 4, 5 and 6 were processed in accordance with the method proposed by Prof. W.I. Odintsow [Odintsow 2010]. This method is based on comparing the tested or designed engine with an ideal one, for which intra-cylinder process parameters and design properties are known. This method can also be used to study different operating modes of an engine, and to model switching the engine to a different fuel grade.

Professor W.I. Odintsow [Odintsow 2010] proposed to use dimensionless criteria to characterise the intra-cylinder processes:

$$B = \left(\frac{\mu_{cp}}{\mu_{ce}}\right)^{1,42} \left(\frac{d_{cp}}{d_{ce}}\right)^{1,05} \left(\frac{P_{fp} - P_{cp}}{P_{fe} - P_{ce}}\right)^{0,71} \left(\frac{\rho_{pp}}{\rho_{pe}}\right)^{1,05} \left(\frac{\sigma_e}{\sigma_p}\right)^{0,37} \left(\frac{\mu_p}{\mu_e}\right)^{0,32} \frac{P_{ce} T_{cp} J_{cp} \theta_{cp}}{P_{cp} T_{ce} J_{ce} \theta_{ce}} \quad (2)$$

$$C = \frac{tg \gamma_p (tg \gamma_p + \cos^{-1} \gamma_p)}{tg \gamma_e (tg \gamma_e + \cos^{-1} \gamma_e)} \quad (3)$$

$$D = \frac{\tau_{ind p} \tau_{wtr e}}{\tau_{ind e} \tau_{wtr p}} \left( \frac{\tau_{Zp}^{-0,5} \tau_{wtr p}}{\tau_{Ze}^{-0,5} \tau_{wtr e}} \right)^{1,6} \quad (4)$$

where:

- $\mu_c$  – injector flow rate,
- $J_c$  and  $d_c$  – number and diameter of injector holes,
- $P_f$  – mean fuel injection pressure,

$P_c$  and  $T_c$  – pressure and temperature of air medium in the cylinder during injection,  
 $g_c$  – cycle fuel dose,  
 $\rho$ ,  $\sigma$  and  $\mu$  – density, surface tension factor and dynamic viscosity of fuel,  
 $\gamma$  – fuel stream angle (Fig. 7),  
 $\tau_{ind}$  – induction period duration,  
 $\tau_{wtr}$  – injection duration,  
 $\tau_z$  – combustion duration.

Parameters with the “p” index apply to the test or designed engine, while parameters with the “e” index – to the ideal engine.

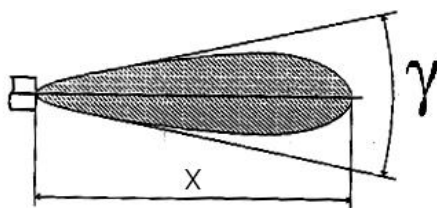


**Fig. 7.** Fuel stream geometry; x – stream length,  $\gamma$  – stream angle

Geometric characteristics of the fuel stream (Fig. 7) can be calculated, for example, using the professor A.S. Lyshevski [Lyshevski 1971] method, in the following sequence:

1. Mean velocity of fuel flow from the injector opening:

$$U_1 = \mu_c \sqrt{2 * 10^4 \frac{g}{\rho_p} (p_p - p_c)}, \quad (5)$$

where:

$g = 9.81$  [m/s<sup>2</sup>],  
 $\rho_p$  – fuel density [kg/m<sup>3</sup>],  
 $p_p$  – mean fuel pressure during injection [bar],  
 $p_c$  – mean pressure of the medium in the cylinder during injection [bar];

2. We (Weber number) and M dimensionless criteria, which characterise the motion of the stream, as well as fuel properties and the density ratio of air in the cylinder to fuel:

$$We = \frac{U_1^2 \rho_p d_c}{\sigma}, \quad (6)$$

$$M = \frac{\mu_p^2}{\rho_p d_c \sigma}, \quad (7)$$

$$\rho = \rho_{pow} / \rho_p. \quad (8)$$

where:

- $U_1$  – mean fuel flow ratio [m/s],
- $d_c$  – mean injector opening diameter [m],
- $\sigma$  – fuel surface tension factor [N/m],
- $\mu_p$  – fuel dynamic viscosity [N\*s],
- $\rho_{pow}$  – air density in the engine cylinder during injection [kg/m<sup>3</sup>];

3. Mean volumetric fuel expenditure during injection:

$$Q = 0.785d_c^2U_1 \quad (9)$$

4. Injection duration

$$\tau_{wtr} = g_c / (\rho_p Q), \quad (10)$$

where  $g_c$  – cycle fuel dose, kg.

5. Fuel stream length:

$$x = \frac{d_c}{\sqrt[4]{2} \sqrt{3}} \left( \frac{U_1 \tau_{wtr}}{d_c} \right)^{0,5} \frac{W_g^{0,105} M^{0,08}}{\rho^{0,5}} \quad (11)$$

6. Fuel cone angle:

$$\gamma = 19,77C_\alpha \mu_c^{0,64} (p_p - p_c)^{0,32} (p_c / p_o)^{0,5} (d_c^{0,39} / \rho_p^{0,43}) (\sigma^{0,07} / \mu_p^{0,14}) (T_o / T_c)^{0,5}, \quad (12)$$

where:

- $C_\alpha = 0.91$  – proportionality factor,
- $\mu_c$  – injector opening expenditure ratio, pressure expressed [kPa],
- $p_o = 100$  kPa – atmospheric pressure,
- $T_o$  – external air temperature.

The angle is expressed in degrees.

The relations between measured soot emissions and dimensionless intra-cylinder process criteria are shown in Figures 8–10.

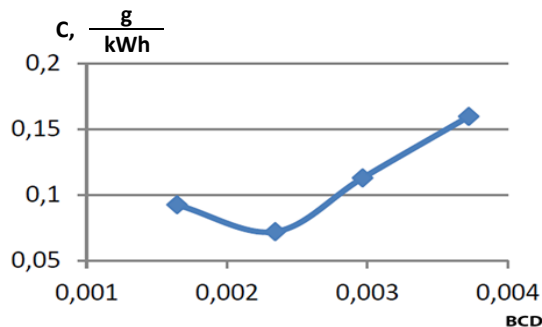


Fig. 8. Measured soot emission relation to the product of BCD criteria for the 3D6 engine



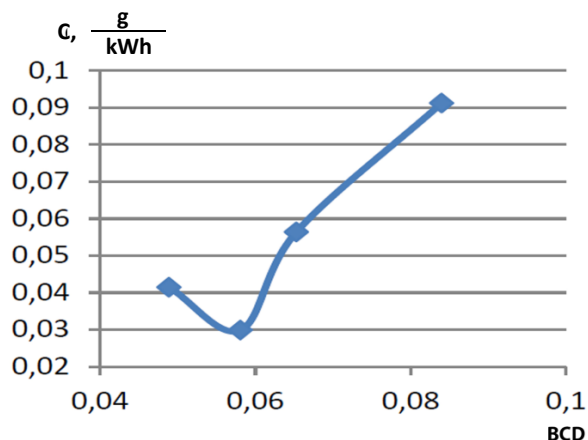


Fig. 9. Measured soot emission relation to the product of BCD criteria for the MAN D 2866 LXE engine

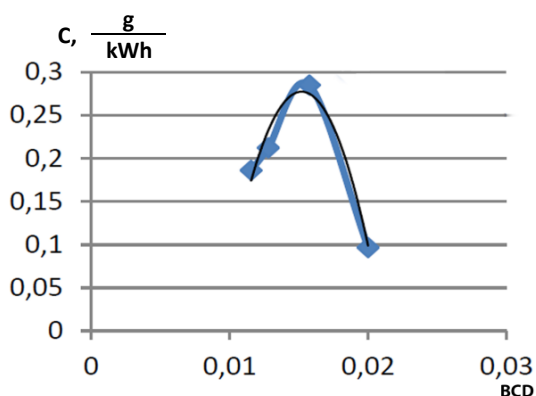


Fig. 10. Measured soot emission relation to the product of BCD criteria for the 6CZN18/22 "Khabarovets" engine

Figures 8–10 show extremes: maximum for the 6CZN18/22 engine, minima for the others. Fuel stream length calculations (equations (5)–(12)), conducted in accordance with the method of Prof. A.S. Lyshevski [Lyshevski 1971] indicated that at extremes, fuel streams reach the piston bottom, and the air fuel mixture is formed using the volumetric/film-based mechanism.

For volumetric formation of air fuel mixture, we have prepared an equation for calculating soot emissions in exhaust gases [Odintsov, Glazkov and Sviridiuk 2017]:

$$\frac{c_p}{c_\varepsilon} = H \left( \frac{J_{c\varepsilon}}{J_{cp}} \right)^{0,4} \left( \frac{d_{c\varepsilon}}{d_{cp}} \right)^{0,8} \left( \frac{g_{c\varepsilon}}{g_{cp}} \right)^{-0,4} \left( \frac{P_{p\varepsilon}}{P_{pp}} \right)^{0,3} \left( \frac{C_\varepsilon}{C_p} \right)^{0,08} \left( \frac{\alpha_\varepsilon}{\alpha_p} \right)^{-0,08} \left( \frac{Q_\varepsilon}{Q_p} \right)^{-0,1} \quad (13)$$

where:

$$H = \left( \frac{\tau_{z\varepsilon} n_{\varepsilon} z_p}{\tau_{zp} n_p z_{\varepsilon}} \right)^{0.12} - \text{duration criteria for intra-cylinder processes,}$$

$n$  – crankshaft rate,

$z$  – engine stroke index ( $z = 1$  for two-stroke and  $z = 0.5$  for four-stroke),

$\alpha$  – excess air ratio,

$Q$  – fuel calorific value,

$C$  – geometric criterion of the fuel stream (equation (3)).

At the volumetric/film-based air fuel mixture formation section, the soot emission measurement results were processed against criteria B and C [Odintsov 2010] (equations (2) and (3)). The processing results are shown in Figures 11–13.

As can be seen in Figures 11–13, specific soot emission value changes at the volumetric/film-based section are described by a power function close to a quadratic parabola.

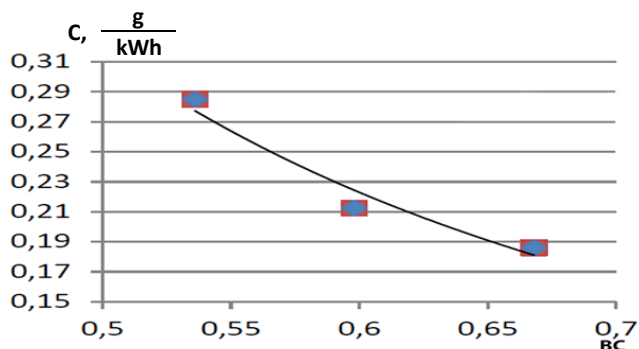


**Fig. 11.** Measured soot emission relation to the product of BC criteria for the 6CZN18/22 "Khabarovets" engine at the volumetric/film-based air fuel mixture formation section

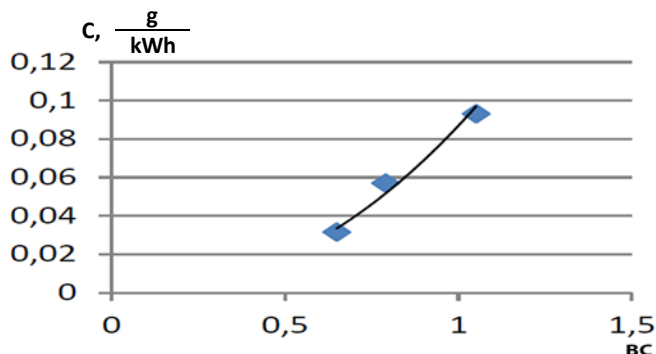


**Fig. 12.** Measured soot emission relation to the product of BC criteria for the MAN D 2866 LXE engine at the volumetric/film-based air fuel mixture formation section

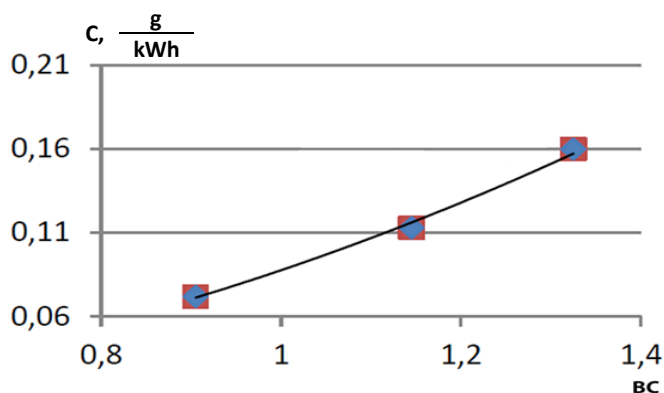


**Fig. 13.** Measured soot emission relation to the product of BC criteria for the 3D6 engine at the volumetric/film-based air fuel mixture formation section

Specifically for the 6 CZN 18/22 engine, the soot emission relation to criteria B and C looks as follows:

$$c = 0.0829(BC)^{-1.937} \quad (14)$$

for the MAN D 2866 LXE engine

$$c = 0.0877(BC)^{2.206} \quad (15)$$

for the 3D6 engine

$$c = 0.087(BC)^{2.078} \quad (16)$$

#### 4. RESULTS

1. The nature of the soot emission process depends on the combustion chamber design.
2. In engines with in-piston combustion chambers, for example 6CZN 18/22, soot emission volume will be reduced when air fuel mixture is formed through the volumetric/film-based mechanism.
3. In engines with indivisible combustion chambers, e.g. MAN D 2866 and 3D6, soot emission volume increases with volumetric/film-based air fuel mixture formation.
4. Empirical equations defining the relations of soot emission volumes to factors in effect during volumetric/film-based air fuel mixture formation have been determined for the test engines.

## REFERENCES

- Bratkov, A.A. (ed.), 1985, *Theoretical Basics of Engine Chemistry Science*, Himiya, Moscow, Russia.
- Broze, D.D., 1969, *Combustion in Piston Engines* (Spalanie w silnikach tłokowych), Maszynostrojenije, Moscow, Russia.
- Dyachenko, N.H., Kostin, A.K., Pugachyow, B.P., Rusinow, R.V., Melnikov, G.V., 1974, *Combustion Engine Theory* (Teoria silników spalinowych), Dyachenko N.H. (ed.), Maszynostrojenije, Leningrad, USSR.
- Kamfer, G.M., 1974, *Heat Exchange and Evaporation Processes During Air Fuel Mixture Formation in Diesel Engines* (Procesy wymiany ciepła i parowania przy wytwarzaniu mieszanki w silnikach Diesla), University of Moscow, Moscow, USSR.
- Kavtaradze, R.Z., 2008, *Piston Engine Theory. Special parts* (Teoria silników tłokowych. Części specjalne), E. Bauman MGTU Publishing House, Moscow, Russia.
- Lyshevski, A.S., 1971, *Fuel Atomisation in Ship Engines* (Rozpylanie paliwa w silnikach okrętowych), Sudostrojenije, Leningrad, USSR.
- Medvedev, G.V., 2016, *Improving Ship Engine Exhaust Gas Treatment System Efficiency Using Metaloceramic Filters* (Powiększenie wydajności systemów czyszczenia gazów odlotowych silników okrętowych przy pomocy filtrów metaloceramicznych), G.V. Medwedew – I.I. Polzunov, Altai State Technical University, Barnaul, Russia.
- Odintsov, W.I., 2010, *Ship Engine Operating Processes. A Monograph*, (Roboczy proces silników okrętowych. Monografia), BGARF Publishing House, Kaliningrad, Russia.
- Odintsov, W.I., Glazkov, D.Y., 2014, *Selected Soot Production Regularities in Ship Engine Cylinders* (Niektóre regularności wytwarzania sadzy w cylindrach silników okrętowych), Vestnik AGTU, Marine Engineering and Technology Series, no. 3, pp. 83–87, Astrakhan, Russia.
- Odintsov, W.I., Glazkov, D.Y., 2016, *Ensuring Safe Ship Engine Operation Conditions by Limiting Incomplete Fuel Combustion Production Emissions* (Zapewnienie bezpiecznych warunków eksploatacji silników okrętowych limitacją emisji produktów niepełnego spalania paliwa), Vestnik AGTU, Marine Engineering and Technology Series, no. 4, pp. 70–79, Astrakhan, Russia.
- Odintsov, V., Glazkov, D., Sviridiuk, N., 2017, *Regularities of Changes in Specific Carbon and Nitrogen Oxide Emissions of Marine and Transport Diesel Engines*, 18-th Annular General Assembly of the International Association of Maritime Universities. Global perspectives in MET: Towards Sustainable, Green and Integrated Maritime Transport, vol. I, pp. 470–480, Varna, Bulgaria.